Collision- and stochastic-fluctuation-induced Hanle resonances in four-wave light mixing in samarium

Y. H. Zou* and N. Bloembergen
Division of Applied Sciences, Harvard University, Cambridge, Massachusetts 02138
(Received 21 March 1986)

A broadband multimode dye laser, detuned from the $\lambda=570.68$ nm resonance line of Sm atoms, was used to provide three incident beams in the standard phase-conjugate four-wave-mixing geometry. The phase-conjugate output intensity was measured as a function of polarization and external magnetic field configurations, and of the pressure of several buffer gases. We have confirmed the theoretical prediction that correlated stochastic fluctuations in the incident light field make a contribution to the four-wave-mixing signal. Collisional cross sections for reorientation among the m sublevels in the $J=1$ ground state of Sm have been obtained for He, Ar, and Xe. Differences in polarization characteristics between the collision-induced Hanle resonances in Na and Sm are pointed out.

I. INTRODUCTION

In this paper the investigation of collision-induced Hanle resonances in four-wave light mixing, previously reported[1] for Na, is extended to Sm vapor with He, Ar, or Xe buffer gas. In Ref. 1 the relationship between induced Zeeman coherences and transverse-optical pumping was discussed in detail. The distinguishing feature in collision-induced coherence or collision-enhanced optical pumping[2,3] is that the detuning $\Delta=\omega-\omega_{ng}$ from the one-photon resonance line is kept large compared with Doppler broadening, collisional damping, Rabi frequencies, and hyperfine interactions. In this regime the four-wave-mixing signal is an increasing function of buffer-gas pressure. The detailed pressure dependence of both the width and peak intensity of the Hanle-type resonances is quite striking. The complexity of the theoretical interpretation of the experimental data is much reduced in comparison with on-resonance four-wave-mixing signals. There is an extensive literature on the latter subject, with particular emphasis on the polarization characteristics of the four waves.[4–9]

The situation in samarium is significantly different from that in sodium vapor, as the ground-state configuration of samarium is a triplet state, $4f^6 6S^2\,{}^7F_1$. The sublevels of the ground state will be denoted by $|g\rangle=|+\rangle$, $|0\rangle$, and $|-\rangle$. The excited state $|n\rangle$ for the resonance at $\lambda=570.68$ mm is the singlet configuration $4f^6 6s6p\,{}^7F_0$. The four pertinent energy levels and relative optical transition probabilities are shown in Fig. 1. Solutions of the density-matrix equations for such a four-level system subjected to two or more light fields are available in the literature.[10,11]

A standard four-wave-mixing geometry, reproduced in Fig. 2, and used extensively in the case of Na, also produced collision-induced Hanle-type resonances in Sm vapor. Two beams of about equal intensity, $|E_1|^2=|E_2|^2$, are linearly polarized in orthogonal directions, $E_1\hat{\mathbf{z}}$ and $E_2\hat{\mathbf{y}}$, respectively. Both beams propagate nearly parallel to the positive $\hat{\mathbf{x}}$ direction. The wave vectors $\mathbf{k}_1$ and $\mathbf{k}_2$ make a small angle θ with each other, with $\Delta k|=|\mathbf{k}_1-\mathbf{k}_2|=2|k_1|\sin(\theta/2)$. Since the beams have the same frequency, they produce a spatial grating, such that the state of polarization of the resultant monochromatic field varies periodically with period $d=2\pi|\Delta k|^{-1}$, changing from right circular to left circular and back again. Taking the $\hat{\mathbf{x}}$ direction as the axis of quantization, an orientation grating is induced in the ground-state manifold.[1,12] Denote the induced rate of pumping out of $|-\rangle$ state to the excited state with

$$W_{-n}=\hbar^{-2}|\mu|^2|E^-|^2\frac{\Gamma_{ng}}{(\omega-\omega_{ng})^2+\Gamma_{ng}^2}\ . \tag{1a}$$

Similarly, the pumping-out rate from the $|+\rangle$ state is

$$W_{+n}=\hbar^{-2}|\mu|^2|E^+|^2\frac{\Gamma_{ng}}{(\omega-\omega_{ng})^2+\Gamma_{ng}^2}\ . \tag{1b}$$

The state $|0\rangle$ is never pumped out. The relative population in the excited state always remains very small for $Wt_{sp}\ll 1$. The width of the electronic transition is given by

$$\Gamma_{ng}=\frac{1}{2t_{sp}}+c_1 p\ , \tag{2}$$

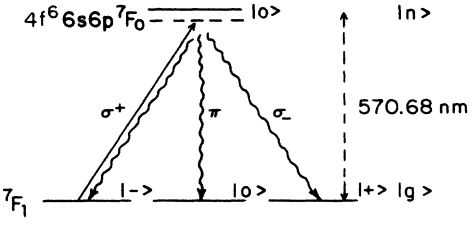

FIG. 1. The four pertinent energy levels of Sm and optical pumping produced by σ^+ light.

 ©1986 The American Physical Society

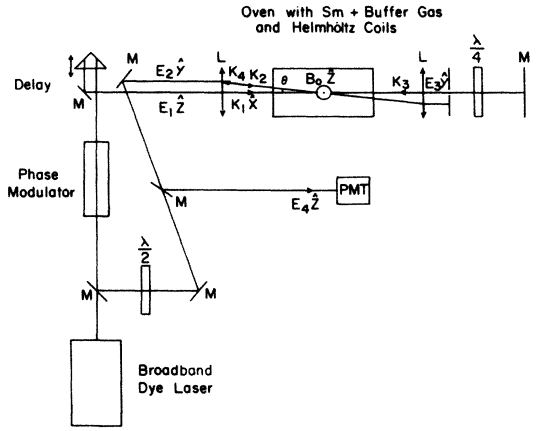

FIG. 2. Diagram of the experimental configuration (M mirrors, L lenses, and PMT photomultiplier tube).

where $c_1 p$ is the collisional contribution to the width of the optical one-photon resonance. The spontaneous lifetime of the $4f^6 6s6p\ ^7F_0$ of Sm has been measured recently by Hannaford and Low,[12] who report the value $t_{sp}=342$ ns. This contrast with a previous result by other authors,[13] $t_{sp}=10.3$ ns. The ground-state manifold gets repopulated by the spontaneous emission in an isotropic fashion. Thus the following rate equations for x directed optical pumping apply:

$$\frac{dN_-}{dt}=-W_+N_-+\tfrac{1}{3}(W_+N_++W_-N_-)$$
$$+\Gamma_{-0}(N_0-N_-)-\Gamma_{-+}(N_--N_+)\,,$$
$$\frac{dN_0}{dt}=+\tfrac{1}{3}(W_+N_++W_-N_-)$$
$$-\Gamma_{-0}(N_0-N_-)-\Gamma_{+0}(N_0-N_+)\,, \qquad (3)$$
$$\frac{dN_+}{dt}=-W_-N_++\tfrac{1}{3}(W_-N_-+W_+N_+)$$
$$+\Gamma_{+0}(N_0-N_+)+\Gamma_{-+}(N_--N_+)\,.$$

We have omitted the diffusion term,[1,12] which will eliminate the population grating in a time t_d it takes a samarium atom to diffuse over the spacing d of the grating.

It is straightforward to write down the steady-state solutions, including optical pump saturation, explicitly, but it is clear on physical grounds that a dipole moment grating proportional to

$$N_+-N_-\propto(W_+-W_-)\propto(|E^+|^2-|E^-|^2)\exp(i\Delta\mathbf{k}\cdot\mathbf{r}) \qquad (4)$$

will be created for weak optical pumping. This induced dipole moment grating in turn scatters a probe beam propagating in the $-\hat{\mathbf{x}}$ direction, with wave vector $\mathbf{k}_3=-\mathbf{k}_1$ giving rise to a phase-conjugate beam with wave vector $\mathbf{k}_4=-\mathbf{k}_2$. If a magnetic field is now imposed in the $\hat{\mathbf{z}}$ direction, the induced dipole moments will start to precess around the $\hat{\mathbf{z}}$ axis, and if the frequencies of the light beams are kept constant, the scattering grating will be averaged out. Thus a Hanle-type resonance in the four-wave-mixing intensity is created with a resonance at $B_0\hat{\mathbf{z}}=0$ and a width determined by $\Gamma_{gg'}\sim\Gamma_{+0}=\Gamma_{-0}\approx\Gamma_{+}$. The intensity of the induced signal for $\Delta\gg\Gamma_{ng}$ will be proportional to Γ_{ng}^2, as is evident from Eqs. (1a) and (1b). Equation (2) shows that the grating is collision enhanced. The contribution from the spontaneous decay alone is comparatively small and does not give rise to an observable signal. Now Γ_{ng} may be regarded as a stochastic fluctuation in the resonant frequency ω_{ng} of the material system. Since Eqs. (1a) and (1b) contain the combination $\omega-\omega_{ng}$, it may be conjectured that stochastic fluctuations in the laser frequency might lead to a similar enhancement. This is indeed the case, as has been analyzed in detail by Prior *et al.* for the case of four-wave light mixing.[14] They denoted the effect with the acronym SFIER for stochastic-fluctuation-induced extra resonances.

This paper presents experimental evidence for this new effect, and detailed results are given for the intensity and width of the Hanle resonances of the Sm atom in four-wave-mixing, as a function of the pressure of several buffer-gases (He, Ar, and Xe) and for various polarization geometries. In Sec. II the essential experimental features are reviewed. Section III presents the results for the linewidth from which the cross section for orientation-changing collisions in the $J=1$ ground-state of samarium with He, Ar, and Xe are derived. In Sec. IV the parametric intensity variations reveal the SFIER effect. In Sec. V the polarization selection rules are discussed. Throughout the paper a comparison with the corresponding results, previously reported for Na, is made and important differences are pointed out.

II. EXPERIMENTAL METHOD

The experimental arrangement is similar to that used[1] for Na and shown in Fig. 2. A new oven, made of stainless-steel tubing, was constructed to sustain temperatures up to about 900 °C. In most of the experiments the oven was heated to about 800 °C, corresponding to a density of Sm atoms of about 10^{14} cm^{-3}. Natural samarium contains a mixture of seven isotopes, and the isotopic shifts have been determined.[15] Our detuning Δ is measured from the center of gravity of the optical line at $\lambda=570.68$ nm. The maximum spread of the isotopic resonances of ^{154}Sm and ^{144}Sm is about 6 GHz. Two odd isotopes, ^{147}Sm, with relative abundance of 14.97%, and ^{149}Sm, with relative abundance of 13.85%, each have a nuclear spin $I=\frac{7}{2}$. The hyperfine structure of their $^7F_1$ ground-state is well known.[16] In our experiments Δ was always larger than this hyperfine splitting and the isotopic shifts, as well as the Doppler width of the $\lambda=570.68$ nm resonance line.

The coherent dye laser was operated with Rhodamine 560 dye and with the etalons in the cavity removed. This increased the power output available near $\lambda=570$ nm, but this output power is then distributed over a large number of statistically independent longitudinal modes with fluc-

tuating phases.

It is well known that two beams with phase fluctuations and a broadband chaotic characteristic, derived from the same laser by a beam splitter, can be used to excite very narrow Raman-type resonances.[17,18] In fact, the narrow Hanle resonances obtained by us[1] for Na had a linewidth of 10 kHz, orders of magnitude narrower than the residual width of the power spectral density of 1 MHz of the laser beams used. This same point was demonstrated earlier by Mlynek *et al.* for Zeeman coherences in Na vapor detected by optical polarization spectroscopy.[19] It is a necessary condition that the difference in optical paths of the light beams, derived from a broadband chaotic laser field, remain smaller than the coherence length of the source. In fact, this condition may be used to measure this coherence length. For this purpose the Hanle resonance experiment in Na vapor was repeated with a broadband dye laser. The optical path length between the two forward beams, with wave vectors $\mathbf{k}_1$ and $\mathbf{k}_2$, respectively, was varied. The Hanle resonance was recorded as a function of the time delay, as shown in Fig. 3. The other experimental parameters are listed in the caption. It is seen that the peak intensity is a function of the delay time. It is a maximum for zero delay time and disappears for delays exceeding 40 ps. A full width at half maximum (FWHM) power bandwidth for the chaotic field of the multimode laser of 7.65 GHz is derived from this curve. The zero time delay can readily be found experimentally by maximizing the four-wave-mixing signal. It was verified that the width of the Hanle resonance itself, observed by varying the external field $B_0\hat{z}$, did not change as a function of time delay. It is also possible to give one of the beams a coherent phase modulation, superimposed on the chaotic one, with an external electro-optic modulator. The narrow Hanle and Zeeman resonances for Na vapor obtained with a broadband chaotic laser field, are shown in Fig. 4. The observed width of 54 kHz is the same as that for a single-mode laser experiment, if the other experimental conditions are the same. It is determined by a combination of magnetic field inhomogeneity, residual Doppler broadening, and power broadening, as discussed previously.[1]

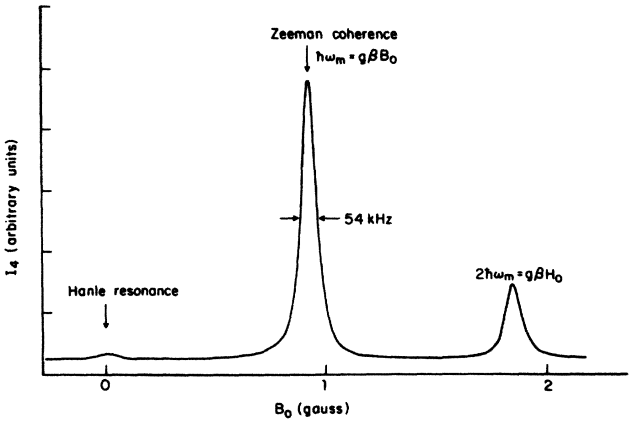

FIG. 4. The Hanle and Zeeman resonances in Na vapor for four-wave light mixing with broadband chaotic fields. The phase modulation frequency is $\omega_m/2\pi = 600$ kHz and the modulation depth was such that $I_1(\omega) = 0.03$ W/cm^2 at (ω), $+0.2$ W/cm^2 at $(\omega \pm \omega_m)$, $+0.08$ W/cm^2 at $(\omega \pm 2\omega_m)$. ($\theta = 0.06°$, $T_{\text{oven}} = 285$ °C, $\Delta/2\pi = 50$ GHz below $^2P_{1/2}$, argon pressure 3260 Torr).

The advantage of the multimode operation is that the observed fluctuations in the nominal power of the laser beam are reduced. Thus the signal-to-noise ratio is improved, as the amplitude fluctuation power spectral density is reduced, presumably due to averaging of the partial power fluctuations in individual modes.

Figure 5 shows the corresponding Hanle and Zeeman resonances obtained with Sm vapor, with natural isotopic composition. The modulation frequency was taken as $\omega_m/2\pi = 10$ MHz, and the modulation depth was adjusted

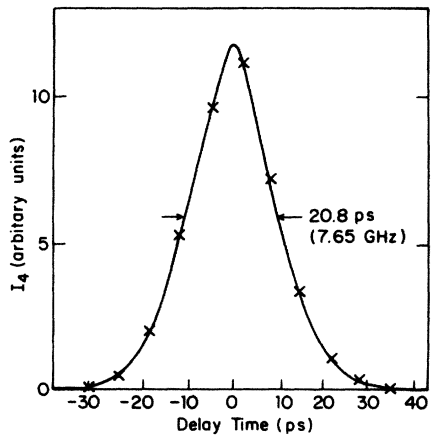

FIG. 3. The Hanle signal in Na vapor in four-wave light mixing with broadband chaotic fields, as a function of the time delay between beams $\mathbf{k}_1$ and $\mathbf{k}_2$ ($\theta = 0.45°$, $T_{\text{oven}} = 230$ °C, $\Delta/2\pi = 40$ GHz below $^2P_{1/2}$, $p(\text{Ar}) = 1000$ Torr, and $I_1 = I_2 = 0.2$ W/cm^2).

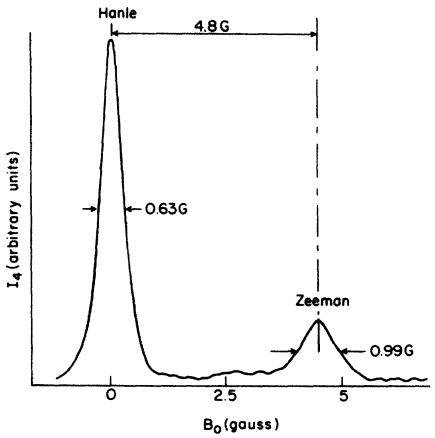

FIG. 5. The Hanle and Zeeman resonances in Sm vapor for four-wave light mixing with broadband chaotic fields. The phase modulation frequency is $\omega_m/=10$ MHz. The intensity distribution is approximately $I_1(\omega) = 0.5$ W/cm^2 at ω, $+0.25$ W/cm^2 at $(\omega \pm \omega_m)$ ($\theta = 0.4°$, $T_{\text{oven}} = 860$ °C, $\Delta/2\pi = 20$ GHz below $\lambda = 570.68$ nm, helium pressure 310 Torr).

so that the combined power in the sidebands at $\omega \pm \omega_m$ was about equal to that of the carrier frequency at ω. The Zeeman resonances occur in a field of 4.8 G for $g\beta B_0 = \hbar\omega_m$. This corresponds to a Lande g factor $g = 1.5$, for the $^7F_1$ state, in good agreement with more precise spectroscopic data.[16] It should be noted that this value applied only to the even isotopes of Sm. In small external fields the g value of the hyperfine states of the odd isotopes with $I = \frac{7}{2}$, coupled to the $J = 1$ electronic momentum, is much smaller. Thus, only the even isotopes with about 70% combined abundance contribute to the Zeeman sidebands. The width of the Zeeman resonances is measured to be about 1.5 times the width of the Hanle resonance. Putting the above-mentioned factors together, and realizing that the two Zeeman sidebands merge into one central component, one may expect the ratio of the peak intensities of Zeeman and Hanle resonances to be given by the factor $0.7 \times 0.5/1.5 \approx 0.22$, in reasonable agreement with the experimental result shown in Fig. 5.

III. LINEWIDTH OF HANLE RESONANCES IN Sm

In the investigation of Na the following contributions to the linewidth have been identified: residual Doppler broadening, homogeneous broadening by collisions with the buffer-gas, magnetic field inhomogeneities, and power broadening by the laser beams. The contribution of orientation-changing collisions between Sm atoms in the ground-state vanishes, because the ground-state has no hyperfine splitting and all atoms have the same g value. The total magnetization is conserved in scalar exchange-type collisions. We have verified this by changing the oven temperature from 780 °C to 880 °C. The linewidth was found to be independent of Sm vapor pressure. We have also verified that power broadening is negligible in the Sm experiments. This contribution depends on the intensity in the three light beams[20]

$$\Delta\omega_{\text{power}} = \sum_{i=1}^{3} \frac{2\Omega_i^2 \Gamma_{ng}}{\Delta^2 + \Gamma_{ng}^2} . \tag{5}$$

Here $\Omega_i = \frac{1}{2}\hbar^{-1} |\mu| |E_i|$ is the Rabi frequency associated with transitions to the excited state $|n\rangle$ induced by beam i. The broadening may be interpreted as a lifetime shortening of the ground-state levels produced by the pumping-out rates, given by Eqs. (1a) and (1b). This contribution was determined by using maximum laser intensities $I_1 = I_2 = 1$ W/cm^2, and minimum detuning $\Delta = 0$, at 300-Torr He pressure. A maximum power broadening of 90 mG was observed under these conditions. The maximum field inhomogeneity over the interaction region was determined by Zeeman coherence experiments on Na, which generally displays narrower resonance. For a field of 2 G produced by the Helmholtz coils, the contribution to the linewidth from such inhomogeneities is les than 20 mG. The resonances displayed by samarium, carried out with a detuning $\Delta > 10$ GHz, usually have widths larger than 400 mG. Examples are given in Figs. 6–8 for the width of Hanle resonance in samarium as a function of partial pressure in the buffer-gases He, Ar, and Xe. It is seen that residual Doppler broadening is only important at low pressures, and there is a large domain of operating conditions where the width of resonance is proportional to the buffer-gas pressure.

It may be concluded from the negligible contribution of the power broadening that in this series of experiments on Sm the weak power regime with $W_{\pm} \ll \Gamma_{gg'}$ prevails. In this regime saturation effects are not important, and lowest-order perturbation theory should provide a good description. Turning the axis of quantization by 90° from the $\hat{\mathbf{x}}$ direction, in which the light beams propagate, to the $\hat{\mathbf{z}}$ direction, in which the external magnetic field is applied, the spatial orientation grating is then described by the Zeeman coherences ρ_{+0} and ρ_{0-}, instead of the x directed population difference $N_+ - N_-$.

A second-order coherence grating is given by

$$\rho_{+0}^{(2)} = \frac{\mu_{n+}\mu_{0n}E_1E_2^*}{4\hbar^{-2}[\hbar^{-1}g\beta B_0 - (\omega_1-\omega_2) + (\mathbf{k}_1-\mathbf{k}_2)\cdot\langle \mathbf{v}_{\text{th}}\rangle - i\Gamma_{g'g}]} \left[\frac{\Delta(\rho_{++}^{(0)} - \rho_{00}^{(0)})}{\Delta^2+\Gamma_{ng}^2} - \frac{i\Gamma_{ng}(\rho_{++}^{(0)} + \rho_{00}^{(0)})}{\Delta^2+\Gamma_{ng}^2} \right]$$

$$\times \exp[i(\mathbf{k}_1-\mathbf{k}_2)\cdot\mathbf{r} - i(\omega_1-\omega_2)t] \tag{6}$$

and a similar expression for ρ_{0-}. Since the initial populations of the nearly degenerate states are equal, only the second term in the large parentheses remains. The intensity of the phase-conjugate four-wave-mixing signal is proportional to the absolute square of the coherence given by Eq. (6). The diffusion-limited, motionally narrowed residual Doppler broadening gives a contribution to the Lorentzian profile,[1] which is additive to the lifetime contribution to the width Γ_{gg}. This Lorentzian shape must be convoluted with the inhomogeneous distribution of the magnetic field inhomogeneities. If the latter can be approximated by a Lorentzian near the line center, a Lorentzian profile as a function of the external field B_0 results. It leads to a line shape for the Hanle resonance,

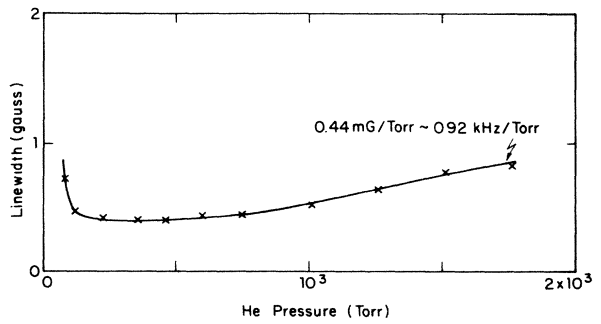

FIG. 6. The linewidth of Hanle resonance of Sm with He pressure ($\theta = 0.3°$, $T_{\text{oven}} = 845$ °C, $I_1 = I_2 = 1$ W/cm^2, and $\Delta/2\pi = -20$ GHz). The solid line is a guide for the eye.

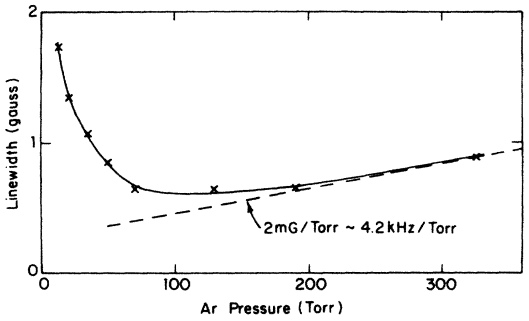

FIG. 7. The linewidth of Hanle resonance of Sm with Ar pressure ($\theta=0.4°$, $T_{\text{oven}}=880°C$, $I_1=I_2=1.6$ W/cm^2, and $\Delta/2\pi=-20$ GHz). The solid line is a guide for the eye.

with $\omega_1=\omega_2$, proportional to

$$\{g^2\beta^2\hbar^{-2}B_0^2+[g\beta\hbar^{-1}(\Delta B_0)+\Gamma_{gg'}+\Delta\omega_{\text{RD}}]^2\}^{-1}, \quad (7)$$

with an effective width

$$\Delta\omega\approx\Gamma_{gg'}+\Delta\omega_{\text{RD}}+\Delta\omega_{\text{inh}}. \quad (8)$$

The first term is proportional to the buffer-gas pressure p, the second term is inversely proportional to pressure, p^{-1}, and the last term is pressure independent. The observed profiles are indeed approximately Lorentzian (compare Fig. 5), and the curves in Figs. 6–8 obey the pressure dependence implied by Eq. (8).

The regime of dominant orientation-changing collisions is defined by the slope of the lines at high buffer-gas pressures, where $\Gamma_{gg'}\gg\Delta\omega_{\text{RD}}$, $\Delta\omega_{\text{inh}}$. It yields the following values for the broadening of the ground-state coherences, with $\Delta m=\pm1$. For Sm-He collisions the rate for orientational change is 0.44 mG/Torr, or 0.92 kHz/Torr; for Sm-Ar 4.2 kHz/Torr; and for Sm-Xe, 7.4 kHz/Torr. These rates are orders of magnitude higher than for Na–noble-gas collisions. This is understandable, as the Sm ground-state is more readily deformable than is the $3\,^2S_{1/2}$ state of Na. Our values are, nevertheless, considerably smaller than those obtained by Mlynek *et al.* with a very different experimental method.[21] They detected radio-frequency resonances by heterodyne Raman light scattering. They reported a rate of about 60 kHz/Torr (45 kHz/mbar) for Sm-He collisions. We cannot explain the very large difference, but point out that the interpretation of the Raman heterodyne result appears to be less direct than that of our data. Neither can we explain why the resonances in a weak external field are almost 50% broader than in zero field, as shown in Fig. 5. One would not expect the relaxation mechanism of Sm–noble-gas collisions to be sensitive to this parameter, and a continuous merging of the two Zeeman resonances into the Hanle resonance in zero field as $\omega_m\to0$ had been expected. A more detailed theoretical analysis of the relaxation mechanisms in the degenerate case $B_0=0$ is desirable.

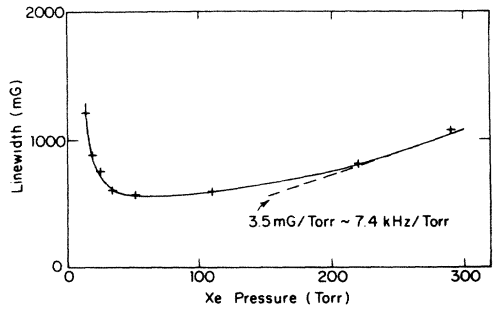

FIG. 8. The linewidth of Hanle resonance of Sm with Xe pressure ($\theta=0.4°$, $T_{\text{oven}}=860°C$, $I_1=I_2=0.8$ W/cm^2, and $\Delta/2\pi=-20$ GHz). The solid line is a guide for the eye.

IV. INTENSITY OF THE HANLE RESONANCE IN Sm

The variation of the integrated Hanle resonance with buffer-gas pressure is shown in Fig. 9. For the previous series of experiments in Na, this integrated intensity was observed to be proportional to the square of the buffer-gas pressure over the whole range. This behavior also follows from the fact that the four-wave-mixing intensity is proportional to the square of the coherence given by Eq. (6). For $\Delta>\Gamma_{ng}$, $\omega_1-\omega_2=0$. This leads to a peak intensity at $B_0=0$ proportional to $(\Gamma_{gg'}+\Delta\omega_{\text{RD}}+\Delta\omega_{\text{inh}})^{-2}\Gamma_{ng}^2$, and an intensity integrated over B_0 proportional to $(\Gamma_{gg'}+\Delta\omega_{\text{RD}}+\Delta\omega_{\text{inh}})^{-1}\Gamma_{ng}^2$. If the experimental width is dominated by $\Delta\omega_{\text{inh}}$ and is independent of pressure, then both the peak intensity and the integrated intensity derive their pressure dependence from $\Gamma_{ng}^2\propto p^2$, as the pressure broadening is always large compared to the spontaneous width proportional to t_{sp}^{-1}. This is the collisional enhancement of the coherence and the four-wave-mixing signal. At low pressures, $\Delta\omega_{\text{RD}}\propto p^{-1}$ becomes important. The integrated intensity then acquires a term proportional to p^3, and the peak intensity acquires terms proportional to p^3 and p^4. This behavior has been observed[1] in Na.

In the present experiments on Sm, the integrated inten-

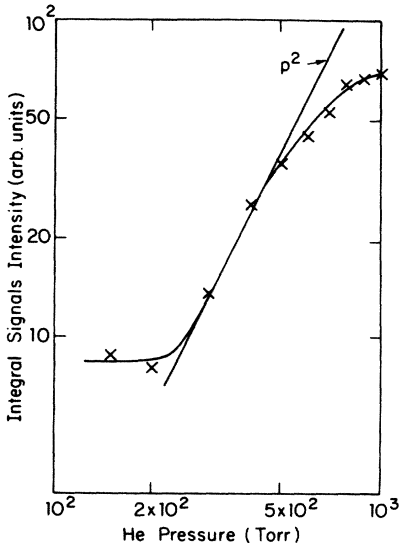

FIG. 9. Integral Hanle four-wave-mixing signal intensity in Sm as a function of helium pressure ($\theta=0.6°$, $T_{\text{oven}}=840°C$, $I_1=I_2=1$ W/cm^2, and $\Delta/2\pi=20$ GHz below $\lambda=570.68$ nm). The solid line is a guide for the eye.

sity versus buffer-gas pressure is shown in Figs. 9 and 10. There is p^2 regime, but at low pressures the intensity appears to become independent of pressure. At very high pressure the intensity may even decrease with increasing pressure. This behavior is quite different from that in the experiments on Na. In the regime at high pressures the condition $\Delta \gg \Gamma_{ng}$ is no longer valid. The detuning $\Delta/2\pi$ could not be chosen larger than 20 GHz because the signal in Sm is weaker and drops as Δ^{-6}. When Γ_{ng} becomes comparable to Δ, the integrated intensity becomes proportional $\Gamma_{gg'}^{-1}[\Gamma_{ng}/(\Delta^2+\Gamma_{ng}^2)]^2$, with both $\Gamma_{gg'}$ and Γ_{ng} proportional to p. Thus, in this regime we first get a linear dependence on p, when $\Gamma_{gg'} \propto p$ and $\Delta \gg \Gamma_{ng}$. For $\Delta \gg \Gamma_{ng}$, this goes over into a p^{-3} behavior. This explains the observed behavior at high buffer-gas pressures in Sm. Note that the behavior for the smaller detuning Δ in Fig. 10 shows the expected decrease at the highest p, whereas the data in Fig. 9, with a detuning twice as large, do not. From Fig. 10 the collision broadening of the optical transition by Sm-He collisions may be estimated as $\Gamma_{ng}/2\pi = 15$ MHz/Torr.

The independence of the intensity from p at low buffer-gas pressures is more interesting. The origin of this effect is attributed to the stochastic fluctuations in the multimode laser field used in these experiments. As argued in the Introduction, for a Lorentzian frequency spectral density, the width of fluctuations Γ_L in the laser frequency may be added to the width Γ_{ng} of the resonance frequency ω_{ng} of the electronic transition. This was put on a firm theoretical basis by Prior *et al.*.[14] The result is that in Eq. (6) Γ_{ng} should be replaced by $\Gamma_L+\Gamma_{ng}$. At low pressures Γ_L is larger than Γ_{ng}, and the integrated intensity, being proportional to $(\Gamma_L+\Gamma_{ng})^2$, is dominated by the Γ_L^2 term, which is independent of buffer-gas pressure. The data in Fig. 3 show that $\Gamma_L \approx 7.6$ GHz.

It cannot be expected that the power spectrum of the free-running multimode dye laser be truly Lorentzian. This shape probably overestimates the spectral density in the far wings, and it is precisely the spectral density at the detuning frequency $\Delta/2\pi \approx 10$–20 GHz which is important. It is noteworthy that the data in Fig. 10, where the detuning is a factor of 2 smaller than in Fig. 9, shows a relative increase in the SFIER-type contribution. The transition from the p independent regime to the p^2 dependence occurs at a higher partial helium pressure (350 Torr for $\Delta/2\pi = 10$ GHz, instead of 250 Torr for $\Delta/2\pi = 20$ GHz).

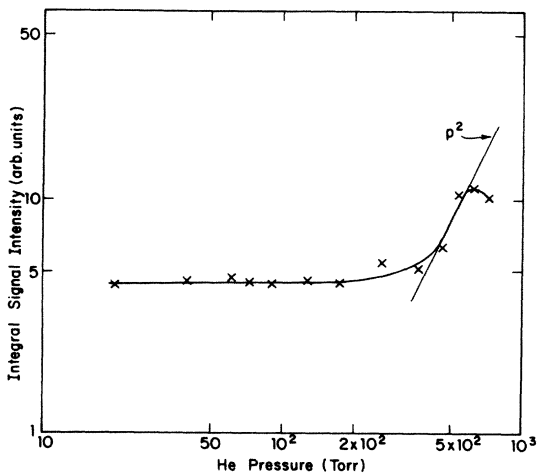

FIG. 10. Integral Hanle four-wave-mixing signal intensity in Sm as a function of helium pressure ($\Delta/2\pi = 10$ GHz below $\lambda = 570.68$ nm), other conditions are the same as in Fig. 9). The solid line is a guide for the eye.

The SFIER-type coherence in four-wave light mixing requires rather large stochastic fluctuations in the laser frequency. It was not possible for us to make more quantitative observations on this effect by using a single-mode cw dye laser in conjunction with an optical phase modulator driven with a large random white-noise voltage. Other investigations have been carried out with this more precise technique to determine the influence of stochastic fluctuations on related nonlinear optical processes, two-photon absorption,[22] and coherent Raman scattering.[23]

The theory for stochastic fluctuations in two-photon nonlinear processes was first developed by Mollow.[24] Agarwal and Kunasz[25] presented a discussion of four-wave light mixing in stochastic fields. The effect we have observed was, however, not contained in that paper but was first predicted by Prior *et al.*,[14] who designated it as SFIER. We believe that the data in Figs. 9 and 10 represent the first experimental confirmation of this new effect.

V. POLARIZATION GEOMETRIES

A comprehensive treatment of polarization properties in phase-conjugate four-wave light mixing has recently been given by Ducloy and Bloch.[4] Earlier these same authors had already discussed polarization selection rules and disorienting collisional effects[5] with special emphasis on the simple case of a $J=0 \rightarrow J=1$ transition, which is applicable to the case of Sm. Agrawal[11] also considered in detail some theoretical aspects characteristic of this situation. These theoretical papers, as well as the early experimental work by Lam and co-workers[6,7] all focused on the resonant condition with $\Delta \approx 0$. This situation is complicated by population trapping in selected velocity groups within the Doppler profile[4] and saturation effects[12,26] due to optical pumping and population trapping.[27] In this sense the investigation of collision-induced effects at large detuning outside the Doppler profile should be easier to interpret. The same symmetry properties and polarization characteristics due to coherences should be expected to hold off-resonance. As we have shown earlier, optical pumping effects are thought to be weak in our series of experiments on Sm, because the weak field limit prevails for $W_{\pm} < \Gamma_{gg'}$. So far, all results obtained were taken with the geometry shown in Figs. 2 and 11(a). If we choose the $\hat{z}$ axis, along which the field B_0 is to be applied, as the axis of quantization, the beam $\mathbf{k}_1$ is π polarized, and beams $\mathbf{k}_2$ and $\mathbf{k}_3$ are σ polarized, i.e., perpendicular to B_0. The phase conjugate beam $\mathbf{k}_4$ is π polarized.

One might superficially think that similar results should be obtained if the backward probe beam $\mathbf{k}_3$ were π polarized, and consequently $\mathbf{k}_4$ would have to be σ polar-

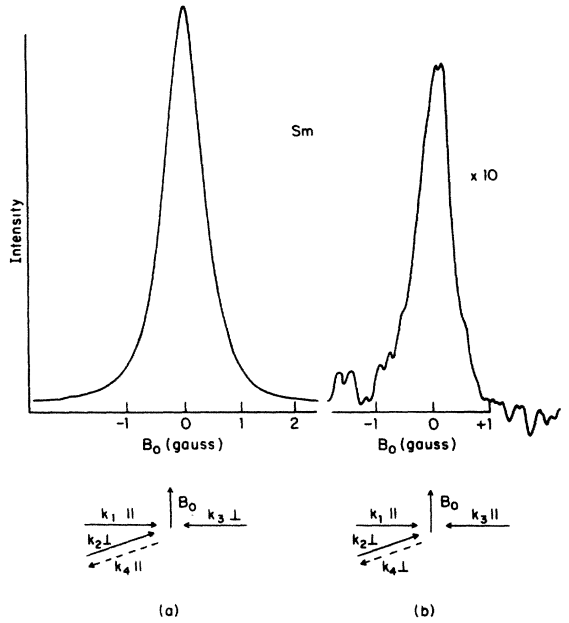

FIG. 11. Hanle resonances in Sm in two different geometries of linear polarization of the backward probe beam ($\theta=0.6°$, $T_{\text{oven}}=860°C$, $I_1=I_2=0.5$ W/cm^2, helium pressure 500 Torr, and $\Delta/2\pi=20$ GHz).

ized. This is, however, not the case. Bloch and Ducloy pointed out[5] that for a $J=0\rightarrow J=1$ transition, with isotropic relaxation of the orientation among the $J=1$ ground-state sublevels, no phase-conjugate signal could occur. The physical argument for this selection rule is that in the four-wave-mixing process one photon is taken out of each of the beams with $\mathbf{k}_1$ and $\mathbf{k}_3$, but in creating the Zeeman coherence $\rho^{(2)}_{0,1}$ proportional to $E_1E_2^*$, one cannot form the required third-order coherence, $\rho^{(3)}_{0,n}$ with the $J=0$ excited state $|n\rangle$, proportional to $E_1E_2^*E_3$, if E_3 is π polarized.

Experimentally we have observed a clear collision-induced Hanle resonance with $\mathbf{E}_3\pi$ polarized parallel to $\mathbf{B}_0$, but the intensity is smaller by more than 1 order of magnitude compared to the case $\mathbf{E}_3\perp\mathbf{B}_0$. Bloch and Ducloy already observed[5] that this selection rule, based on arguments of simultaneous conservation of energy and angular momentum could be broken if collisional reorientation were anisotropic, i.e., if the relaxation time for alignment in the $J=1$ ground state were different from that of its polarization. Such an anisotropy is equivalent to requiring that $\Gamma_{\pm}\neq\Gamma_{+0}=\Gamma_{0-}$ in Eq. (3). Our experimental observation could be explained in terms of such an anisotropic relaxation effect.

It is perhaps instructive to discuss the same situation also from the point of view that the $\hat{\mathbf{x}}$ direction of the propagation of the light beams is the axis of quantization. The beams $\mathbf{k}_1$ and $\mathbf{k}_2$ produce two $\hat{\mathbf{x}}$ directed population gratings, N_+-N_0 and N_0-N_-. These gratings are probed by the linearly polarized probe beam $\mathbf{k}_3$. This probe can be decomposed into two circularly polarized probes. One of these probes the grating involving N_+, the other that involving N_-. For $\mathbf{k}_3$ polarized in the $\hat{\mathbf{y}}$ direction, the diffracted signals from these two gratings interfere constructively to produce the beam $\mathbf{k}_4$. For $\mathbf{k}_3$ polarized in the $\hat{\mathbf{z}}$ direction, the relative phase of the two circularly polarized probes is changed by 180°, and the diffracted signals now interfere destructively in the direction $\mathbf{k}_4$.

Next the polarization geometry in Fig. 12(b) is considered, in which all beams are circularly polarized in the same sense with respect to the laboratory frame. There is population grating in the N_+ state of the $J=1$ manifold setup because the pumping-out rate W_+ from this state is modulated by the intensity interference pattern $|E^+|^2$ of two forward beams, $\mathbf{k}_1$ and $\mathbf{k}_2$. This population grating is probed by the backward beam with the same circular polarization. The relative intensity appears somewhat lower than for the linear polarization case with similar intensity of the light beams. As the first $B_0\hat{\mathbf{z}}$ is applied in the transverse direction, the polarization precesses around the $\hat{\mathbf{z}}$ axis and the grating averages out to zero, if the Zeeman precession frequency is larger than the damping constant $g\beta H_0>\hbar\Gamma_{+0}$. This is the same explanation as used in the original Hanle effect.

This geometry is identical to that used by Köster *et al.*[28] in their experiment on Hanle resonances in Na vapor. We have repeated their experiment but with large detuning and high buffer-gas pressure, as shown in Fig. 13. The collision-induced Hanle resonance shows qualitatively the same behavior as that observed by Köster *et al.*, who used zero or small detuning.[28] At modest power levels of the light beams, optical pumping leads to saturation effects and population trapping in the $\pm\frac{1}{2}$ levels of the ground $3\,^2S_{1/2}$ state. A dip develops at the center of the resonance, $B_0=0$. This should be contrasted with the re-

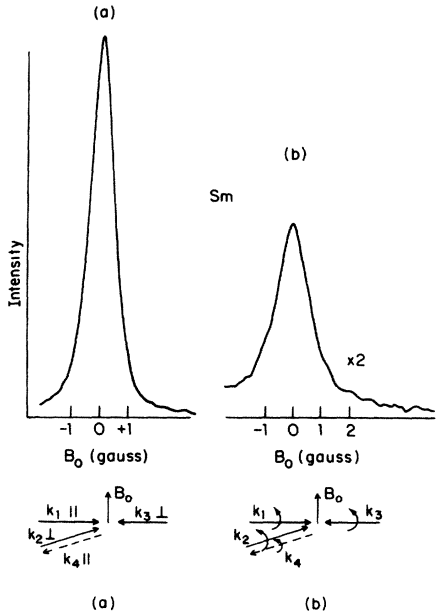

FIG. 12. Hanle resonances in Sm for a geometry with (a) linear polarizations and (b) circular polarizations ($\theta=0.6°$, $T_{\text{oven}}=860°C$, $I_1=I_2=1.4$ W/cm^2, helium pressure 530 Torr, and $\Delta/2\pi=20$ GHz).

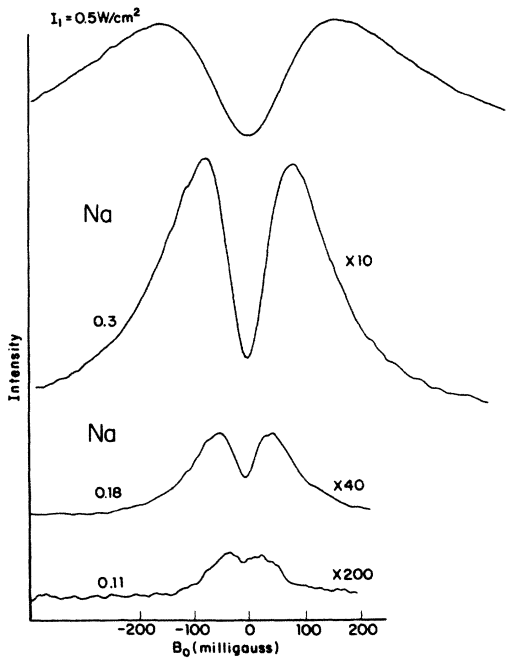

FIG. 13. Hanel resonances in Na vapor, when all beams are right circularly polarized, for various intensities of the light beams, $I_1 = I_2$. The magnetic field is scanned in the transverse direction. The dye laser is single mode ($\theta = 0.6°$, $T_{oven} = 310°C$, partial argon pressure 1260 Torr, $\Delta/2\pi = 50$ GHz above the D_2 resonance).

sults on Sm, where we are evidently in the weak field limit, $W_{\pm} \ll \Gamma_{gg'}$, and no minimum is observed.

Finally the interesting geometry is considered, in which the beams $\mathbf{k}_1$ and $\mathbf{k}_2$ have circular polarizations in the opposite sense, and the magnetic field B_0 is scanned in the longitudinal $\hat{\mathbf{x}}$ direction, parallel to the direction of propagation of the light beams. With this axis of spatial quantization, the two light beams induce a coherence grating $\rho^2_{\pm} \propto E_1 E_2^* \exp[i(\mathbf{k}_1 - \mathbf{k}_2)\cdot\mathbf{r}]$, between the two sublevels with $m = \pm 1$. This is an alignment grating. If the two light beams had the same amplitude, they would produce at each point in space a linearly polarized field, but the direction of this linear polarization varies periodically.

This $\Delta m = 2$ alignment coherence was discussed theoretically by Agrawal[11] and by McLean *et al.*[10] The latter also demonstrated the existence of this coherence by a Hanle-type sharp dip in the resonance fluorescence spectrum of a $J = 0 \rightarrow J = 1$ transition in a Ne discharge,[10] as well as in Sm vapor.[29]

Unfortunately, our four-wave-mixing experiment in this geometry yielded a negative result for either linear or circular polarization of beam 3. This is all the more puzzling, as populating trapping effects in the $|0\rangle$ state should be negligible in the weak field limit, as discussed previously.

VI. CONCLUSION

The collision-induced Hanle resonances in Sm show significant differences from those in Na. We have demonstrated experimentally the SFIER effect predicted theoretically, by the use of a free-running multimode dye laser. The orientation changing collisions in the $J = 1$ ground-state manifold of Sm have much larger cross sections than for the $3\,^2S_{1/2}$ state for Na. New values for such collision cross sections of Sm with He, Ar, and Xe have been obtained. Evidence is presented for some deviation from isotropy, i.e., a difference in the decay constants for alignment and polarization in the $J = 1$ manifold. The observed variations in intensity for different polarization geometries and external magnetic field configurations are only partially understood.

It is possible that some of the noted discrepancies might be caused by contributions from two other Sm resonance lines in the immediate vicinity of the $J = 1 \rightarrow 0$ transition at $\lambda = 570.675$ nm, on which our discussion has focused. Albertson[30] has reported a line at $\lambda = 570.620$ nm, which is $\Delta'/2\pi = 52$ GHz higher in frequency, and another line at $\lambda = 570.772$ nm, or $\Delta''/2\pi = -44$ GHz, lower than the $\lambda = 570.675$ nm line. It appears that the line at the higher frequency corresponds to a $^7F_3 \rightarrow {}^7G_2$ transition between the same electronic configurations, and the line at the lower frequency to a $^7F_2 \rightarrow {}^7I_3$ transition.[31] The latter is weaker in absorption at 850°C than the $\lambda = 570.675$ nm line, while the high-frequency line is the strongest,[30,31] but quantitative oscillator strengths are not known. The g factors[16] of the $^7F_{2,3}$ states are also 1.5, so that these transitions, in principle, make contributions to both the collision-induced Hanle and Zeeman resonances.

The induced coherence contains additional terms of the form given by Eq. (6), corresponding to coherence gratings induced in Sm atoms in the $^7F_{2,3}$ states of the ground electronic configuration. The observed intensity of the collision-induced signal should be proportional to

$$I \propto \left| \frac{C}{\Delta^3} + \frac{C'}{(\Delta - \Delta')^3} + \frac{C''}{(\Delta - \Delta'')^3} \right|^2 . \tag{9}$$

All observations reported in this paper were obtained for detunings in the range 10–20 GHz below the $\lambda = 570.675$ nm resonance, i.e., away from the strongest line at the higher frequency. For $\Delta/2\pi = -10$ GHz, the first term is obviously dominant as the denominator of the second term in Eq. (9), $(\Delta - \Delta')/2\pi = -62$ GHz, is larger by a factor $(6.2)^3$, and the last term is smaller by at least a factor $(3.4)^3$, since $C'' < C$. Thus in a range of detunings near -10 GHz, the signal is proportional to the dominant term, or C^2/Δ^6. Turning now to a larger detuning on the low-frequency side, $\Delta/2\pi = -20$ GHz, the denominator of the last term is only smaller by a factor $(24/20)^3$ than that of the first term. The transition at $\lambda = 570.722$ nm should yield an observable destructive interference in this situation, if C''/C is not too small. Experimentally, the decrease of the observed signal intensity was not faster than Δ^{-6}, as might have been expected in this case of destructive interference between the coherence gratings. Unfortunately, the accuracy of the experimental data in Sm is inferior to the case of Na, where the Δ^{-6} behavior was verified with precision for detunings up to 50 GHz. At large detunings deviations were noted for the case of Na because the impact regime approximation ceased to be valid, and also interference between the D_1 and D_2 resonance lines were observed in that case. It would clearly be

of interest to extend the investigations to larger detunings in Sm and to study the absorption strength and the collision-induced effects of the adjacent resonances near $\Delta=\Delta'$ and Δ'' in more detail. The available data reported in this paper did not reveal an identifiable contribution from the adjacent resonances.

ACKNOWLEDGMENT

This work was supported by the Joint Services Electronics Program of the U.S. Department of Defense under Contract No. N00014-84-K-0465.

*Present address: Department of Physics, Peking University, Beijing, People's Republic of China.

[1]Y. H. Zou and N. Bloembergen, Phys. Rev. A **33**, 1730 (1986); N. Bloembergen, Ann. Phys. (Paris) **10**, 681 (1985). These papers give an historical account of the collision-induced Hanle effect and contain many references to earlier work.

[2]N. Bloembergen, Y. H. Zou, and L. J. Rothberg, Phys. Rev. Lett. **54**, 186 (1985).

[3]L. J. Rothberg and N. Bloembergen, Phys. Rev. A **30**, 820 (1984).

[4]M. Ducloy and D. Bloch, Phys. Rev. A **30**, 3107 (1984).

[5]D. Bloch and M. Ducloy, J. Phys. B **14**, L471 (1981).

[6]J. F. Lam, D. G. Steel and R. A. MacFarlane, Phys. Rev. Lett. **49**, 1628 (1982).

[7]J. F. Lam and R. L. Abrams, Phys. Rev. A **26**, 1539 (1982); D. G. Steel and R. A. MacFarlane, *ibid.* **27**, 1217 (1983).

[8]S. Saikan and M. Kiguchi, Opt. Lett. **7**, 5555 (1982).

[9]M. Ducloy, R. K. Raj, and D. Bloch, Opt. Lett. **7**, 60 (1982).

[10]R. J. McLean, R. J. Ballagh, and D. M. Warrington, J. Phys. B **18**, 2371 (1985).

[11]G. P. Agrawal, Phys. Rev. A **28**, 2286 (1983).

[12]P. Hannaford and R. M. Lowe, J. Phys. B **18**, 2365 (1985).

[13]T. Dohnalik, M. Stankiewicz, and J. Zakrewski, in *Laser Spectroscopy VI,* edited by H. P. Weber and W. Luthy (Springer, Heidelberg, 1983), p. 58.

[14]Y. Prior, I. Schek, and J. Jortner, Phys. Rev. A **31**, 3775 (1985).

[15]J. Bauche, R. J. Champeau, and C. Sallot, J. Phys. B (London) **10**, 2049 (1977). H. Brand, B. Nottbeck, H. H. Schultz, and A. Staudel, *ibid.* **11**, L99 (1978).

[16]W. J. Childs and L. S. Goodman, Phys. Rev. A **6**, 2011 (1972); G. K. Woodgate, Proc. R. Soc. (London) Ser. A **293**, 117 (1966).

[17]J. E. Thomas, P. R. Hemmer, S. Ezekiel, C. C. Lieby, Jr., P. H. Picard, and C. R. Willis, Phys. Rev. Lett. **48**, 867 (1982).

[18]W. E. Bell and A. L. Bloom, Phys. Rev. Lett. **6**, 280 (1961); W. Happer and B. S. Mathur, *ibid.* **18**, 727 (1976).

[19]J. Mlynek, K. H. Drake, G. Kersten, D. Frölich, and W. Lange, Opt. Lett. **6**, 87 (1981).

[20]G. Orriols, Nuovo Cimento B **53**, 1 (1979).

[21]J. Mlynek, Chr. Tamm, E. Buhr, and N. C. Wong, Phys. Rev. Lett. **53**, 1814 (1984).

[22]D. E. Elliott, M. W. Hamilton, K. Arnett, and S. J. Smith, Phys. Rev. Lett. **53**, 439 (1984).

[23]M. Trippenbach, K. Rzazewski, and M. G. Raymer, J. Opt. Soc. Am. B **1**, 671 (1984).

[24]B. R. Mollow, Phys. Rev. **175**, 1555 (1968).

[25]G. S. Agarwal and C. V. Kunasz, Phys. Rev. A **27**, 996 (1983).

[26]D. Bloch and M. Ducloy, J. Opt. Soc. Am. A **73**, 635 (1983).

[27]H. R. Gray, R. M. Whitley and C. R. Stroud, Jr., Opt. Lett. **3**, 218 (1978).

[28]E. Köster, J. Mlynek, and W. Lange, Opt. Commun. **53**, 53 (1985).

[29]R. J. McLean, D. S. Goush, and P. Hannaford, in *Laser Spectroscopy VII,* edited by T. W. Hansch and Y. R. Shen (Springer-Verlag, New York, 1985), p. 220.

[30]W. Albertson, Phys. Rev. **47**, 370 (1935).

[31]W. C. Martin, R. Zahlubas, and L. Hagen, *Atomic Energy Levels: The Rare-Earth Elements,* Natl. Bur. Stand (U.S.) Circ. No. 60 (U.S. GPO, Washington, D.C., 1978).